

# Thermal conductivity and diffusivity of free-standing silicon nitride thin films

Xiang Zhang and Costas P. Grigoropoulos<sup>a)</sup>

*Department of Mechanical Engineering, University of California, Berkeley, California 94720*

(Received 25 March 1994; accepted for publication 17 October 1994)

The thermal conductivity and diffusivity of free-standing silicon nitride (Si-N) films of 0.6 and 1.4  $\mu\text{m}$  in thickness are measured. A new experimental technique, the amplitude method, is proposed and applied to measurement of the thin-film thermal diffusivity. The thermal diffusivity is determined by three independent experimental approaches: the phase-shift method, the amplitude method, and the heat-pulse method. Good agreement among the measured thermal diffusivities obtained by the three methods indicates the validity of the amplitude method. High-resolution electron microscopy studies show a large quantity of voids in the 1.4  $\mu\text{m}$  Si-N films. In contrast, very few voids are found in the 0.6  $\mu\text{m}$  films. This difference may be responsible for the measured lower conductivity of the 1.4  $\mu\text{m}$  Si-N films as compared to the 0.6  $\mu\text{m}$  thin films. © 1995 American Institute of Physics.

## I. INTRODUCTION

As a superior dielectric material, silicon nitride (Si-N) thin film has been used extensively in semiconductor device applications such as surface passivation, oxidation and diffusion masks, capacitors in DRAM, encapsulants for thermal treatments, and gate insulators in metal-insulator semiconductor field-effect transistors (MISFET).<sup>1-6</sup> Most of these films are fabricated by low-pressure chemical vapor deposition (LPCVD) at high temperature about 800 °C. Recent use of Si-N in the microfabrication of sensors and actuators has attracted a lot of attention from the industry as well as academia.<sup>7-9</sup> Thermal design in these devices is becoming increasingly important for improving performance and reliability. However, it is demonstrated that the thin-film thermal conductivity and diffusivity can deviate significantly from its bulk material counterparts, due to differences in microstructure and phonon transport mechanisms between the thin film and the bulk material.<sup>10,11</sup> Knowledge of the thermal properties of Si-N thin film in these applications is therefore essential.

Several experimental techniques have been developed to measure the thermal conductivity and diffusivity of thin-film materials. A modulated calorimeter method has been used to measure the thermal diffusivity of polyimide films of 5 and 10  $\mu\text{m}$  in thickness.<sup>12</sup> In this method, the optical reflectance from the back of a multilayer system is measured while the front face is subjected to modulated laser heating. The reflectance signal carries information about the average temperature of the calorimeter, including a phase shift from which the thermal diffusivity of the thin film deposited on the calorimeter can be extracted. Photothermal displacement interferometry determines thermal diffusivities of amorphous silicon films on substrates by detecting the transient thermal expansion of the film heated by a laser pulse of 550 ns duration.<sup>13</sup> Some experimental ac and dc techniques were applied to the thermal conductivity measurements of semiconducting thin films deposited on substrates, ranging in thickness from na-

nometer to millimeter.<sup>11,14</sup> All the above methods, however, analyzed thin-film thermal properties on substrates. Effects from the substrate and the interface between the thin film and the substrate introduce both inaccuracy for the measured values and complexity for the experimental analysis. The microbridge method has been developed for a more direct measurement of the thermal conductivity of a heavily doped LPCVD polycrystalline silicon film which was elevated by 3  $\mu\text{m}$  above the silicon substrate.<sup>15</sup> In order to eliminate any possible influences from the substrate, it is necessary to design measurements of the thermal conductivity and diffusivity of thin films in a free-standing form.

In the present work, free-standing Si-N films are fabricated. Microdevices are patterned on these films for the thermal conductivity and diffusivity measurement (Fig. 1). The experiments are based on electrical heating and thermistor sensing by microdevices on the free-standing films. Two thicknesses of Si-N films studied in this work are 0.6 and 1.4  $\mu\text{m}$ . A dc current heating provides constant heat flux along the film to establish a steady temperature field. By measuring the temperature at the sensor location, the thermal conductivity of the free-standing film can be found. The thermal diffusivity of the Si-N thin films is determined by three independent methods in the present work: the phase-shift method, the amplitude method, and the heat-pulse method. All the three methods involve transient temperature fields which are strongly dependent on the thermal diffusivity of the Si-N film. The amplitude method is proposed and applied in this work, as a new method to measure thermal conductivity and diffusivity of the thin film. This method can be carried out simultaneously with the phase-shift method. In this paper, a heat-transfer analysis is presented, followed by a discussion of the experimental techniques employed. The Si-N thin-film thermal properties obtained by the different experimental methods are compared.

## II. THERMAL ANALYSIS

To determine the thermal properties of thin Si-N films, a thermal analysis is necessary, providing a theoretical basis

<sup>a)</sup> Author to whom correspondence should be addressed.

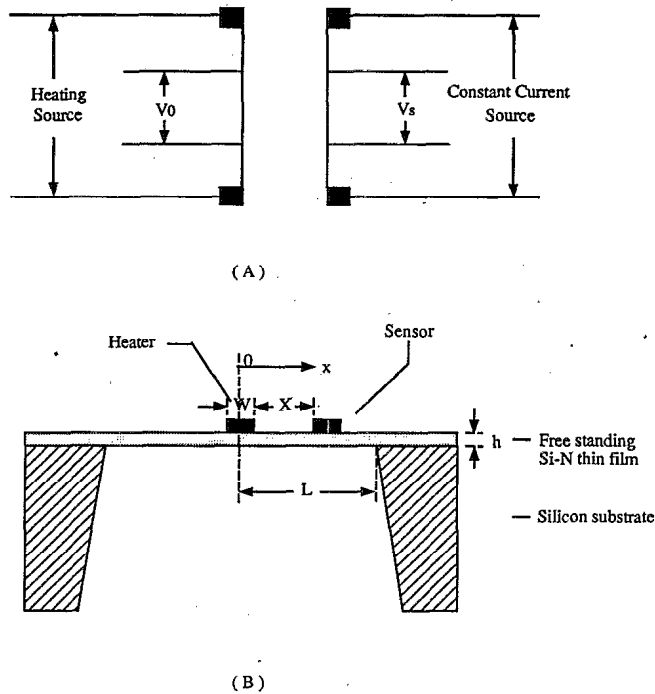


FIG. 1. Schematic diagram of a free-standing Si-N thin film with micro-heater and microsensors: the top view (A) and the side view (B).

for the experiments. In the present work, thermal convection loss is eliminated by performing the experiments in a vacuum chamber of  $10^{-5}$  Torr. A conservative estimation of the thermal emissivity of silicon nitride thin film is about 0.3 based on several previous investigations.<sup>16,17</sup> The temperature error at the sensor location caused by thermal radiation loss is less than 3%. Therefore the thermal radiation loss is negligible in this work. Possible two-dimensional effects caused by the edges of the thin film are investigated numerically. It is found that the thermal properties of the Si-N thin film determined via the one-dimensional (1D) heat-transfer model are in good agreement with those derived using the two-dimensional (2D) model.

### A. Thermal conductivity measurement

As illustrated in Fig. 1, a steady heat flux generated by a dc current passing through the heater which is located at the center of a free-standing thin Si-N film, propagates along the thin film in the  $\pm x$  directions. The heat flux decreases dramatically beyond the edge of the free-standing film where the bulk silicon substrate acts as a large heat sink. It is therefore reasonable to approximate the temperature at the edge as the room temperature  $T_0$ . The steady-state 1D heat-conduction model gives

$$k = \frac{q}{\Delta T}(L - X), \quad (1)$$

where  $k$  is the thin-film thermal conductivity,  $q$  the heat flux,  $T_s$  the temperature at the sensor,  $\Delta T = T_s - T_0$ . The locations of the sensor and the edge of the free-standing film are designated by  $X$  and  $L$ , respectively. The sensor in this experiment is a thin metal strip whose resistivity varies with temperature. With a small constant current passing through this

metal strip, the voltage change across the sensor reflects the temperature changes of the film at the sensor location. With the heat flux  $q$  measured at the heater, and the temperature change  $\Delta T$  measured at the sensor, the thermal conductivity of the thin film can be determined from Eq. (1).

### B. Thermal diffusivity measured by phase-shift method and amplitude method

The phase-shift method has been widely used to measure the thermal diffusivity of thin-film materials.<sup>12,18</sup> A sinusoidal heat flux is generated at the heater in Fig. 1 by applying an ac current. The 1D transient heat conduction can be formulated as

$$\frac{\partial T}{\partial t} = \alpha \frac{\partial^2 T}{\partial x^2}, \quad (2)$$

with an initial condition and boundary conditions:

$$T(x, 0) = T_0, \quad (3)$$

$$T(L, t) = T_0, \quad (4)$$

$$-k \left. \frac{\partial T}{\partial x} \right|_{x=0} = 2A \cos^2 \frac{\omega t}{2} = A(\cos \omega t + 1), \quad (5)$$

where  $A = V_0^2 / (8RhL)$ ,  $V_0$  is the voltage amplitude applied to the heater,  $R$  the electrical resistance of the heater,  $h$  the thickness of the thin film,  $\alpha$  the thermal diffusivity of the thin film, and  $\omega/2$  the heating frequency. The solution for this problem is

$$T(x, t) - T_0 = \frac{A}{k} \sqrt{\frac{\alpha}{\omega}} \exp\left(-\sqrt{\frac{\omega}{2\alpha}}x\right) \times \cos\left(\omega t - \sqrt{\frac{\omega}{2\alpha}}x - \frac{\pi}{4}\right) - \frac{A}{k}(x - L). \quad (6)$$

Boundary condition (4) is reasonably satisfied as the amplitude coefficient in Eq. (6) approaches zero for the experimental parameters employed.

Equation (6) depicts a thermal wave which travels along the  $x$  direction on the Si-N thin film with a phase shift and a decaying amplitude. Two characteristics of the solution can be used to extract the thermal diffusivity or conductivity of the Si-N thin film:

$$\text{phase shift: } \Delta\Phi = \sqrt{\frac{\omega}{2\alpha}}x + \frac{\pi}{4}, \quad (7)$$

$$\text{amplitude: } \text{amp} = \frac{A}{k} \sqrt{\frac{\alpha}{\omega}} \exp\left(-\sqrt{\frac{\omega}{2\alpha}}x\right). \quad (8)$$

For a fixed sensor location, i.e.,  $x = X$ , the thermal diffusivity  $\alpha$  can be obtained from experimental determination of the relationship between the phase shift  $\Delta\Phi$  and the thermal wave frequency,  $\omega$ , based on Eq. (7). Likewise, the thermal diffusivity can be found from the amplitude which decays with increasing wave frequency  $\omega$  at a fixed sensor location, and the known thermal conductivity, according to Eq. (8). These two methods of determining the thermal diffusivity are independent, even though their mathematical formulations are drawn from the same Eq. (6). Hence, some advantages in

determining the thin-film thermal properties can be gained. First, it is possible to simultaneously carry out the two measurements in a single experimental run. Secondly, the measured values of the thermal diffusivity from two methods can be verified with each other if the thermal conductivity is known. Lastly, the thermal conductivity can be deduced from the amplitude method once the thermal diffusivity is found by the phase-shift method. Both the thermal conductivity and the diffusivity of the free-standing thin film can therefore be determined in a single experimental run.

### C. Thermal diffusivity measured by the heat-pulse method

The third way to obtain the thin-film thermal diffusivity is by studying the transient temperature profile following a short heat pulse.<sup>19</sup> A heat pulse is induced by passing an electric current pulse through the heater. This 1D transient problem is formulated as follows:

$$\frac{\partial T}{\partial t} = \alpha \frac{\partial^2 T}{\partial x^2}, \quad (9)$$

with initial and boundary conditions:

$$T(x, 0) = T_0, \quad (10)$$

$$T(L, t) = T_0, \quad (11)$$

$$-k \frac{\partial T}{\partial x} \Big|_{x=0} = \begin{cases} 2A, & 0 < t < t_0 \\ 0, & t > t_0 \end{cases} \quad (12)$$

By separation of variables and superposition principles, an analytic solution can be expressed as

$$T(x, t) - T_0 = \frac{2A}{k} (L - x) + \sum_{n=0}^{\infty} B_n \cos(\lambda_n x) \times \exp(-\alpha \lambda_n^2 t) \quad \text{for } 0 < t < t_0, \quad (13)$$

$$T(x, t) - T_0 = \sum_{n=0}^{\infty} B_n \cos(\lambda_n x) \exp(-\alpha \lambda_n^2 t) [1 - \exp(\alpha \lambda_n^2 t_0)] \quad \text{for } t > t_0,$$

where

$$B_n = -\frac{16AL}{k(2n+1)^2 \pi^2}, \quad \lambda_n = \frac{(2n+1)\pi}{2L},$$

and here  $t_0$  is the heat-pulse duration. The experiments aim to measure the transient temperature profile at the sensor position, both during and after the heat-pulse generation. A numerical code is developed, based on Eq. (13), to fit the experimental temperature profile by varying the thermal diffusivity  $\alpha$ . The best fit gives the thermal diffusivity of the thin film.

### III. EXPERIMENTS

Si-N thin films are fabricated in the Microfabrication Laboratory at the University of California at Berkeley. These films are deposited on single-crystal silicon wafers in a low-pressure chemical vapor deposition (LPCVD) furnace. The

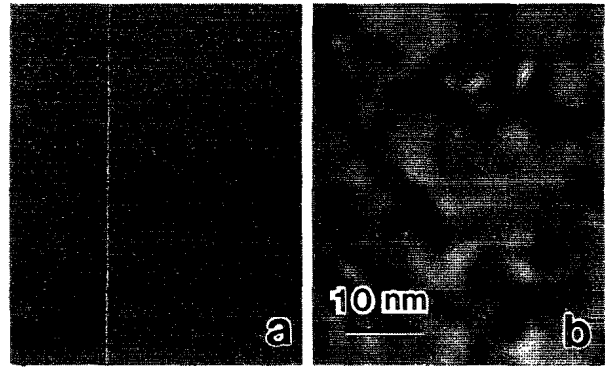


FIG. 2. High-resolution electron microscopy of the Si-N films with a thickness of (a) 0.6  $\mu\text{m}$  and (b) 1.4  $\mu\text{m}$ .

deposition is made at a temperature of 835  $^{\circ}\text{C}$  and a pressure of 140 mTorr. The deposition rate is about 40  $\text{\AA}/\text{min}$ . Following a backside patterning on the wafer, plasma is introduced to etch out a  $2 \times 2 \text{ mm}^2$  square of Si-N, while the rest of the thin film on the backside is used as a protective layer. Bulk single-crystal silicon is etched away from the square at the backside of the wafer in a KOH solution at 80  $^{\circ}\text{C}$ , leaving a free-standing Si-N thin film on the front side as shown in Fig. 1. After sputtering a 2000  $\text{\AA}$  tungsten layer on top of the free-standing Si-N film, the lithography is carried out on the wafer by a wafer stepper. The patterned tungsten layer is then etched in a hydrogen peroxide solution (30%) at room temperature. It is critical to completely etch the tungsten film till the Si-N film, leaving only the masked part. Finally, the free-standing Si-N film with the patterned devices is cut from the silicon wafer and bound to a 24-pin packaging chip with silver wires 25  $\mu\text{m}$  in diameter. Extensive cleaning procedures are taken at each processing step to ensure that both sides of the thin Si-N films remain free from residue. The thicknesses of the Si-N films are measured by an ellipsometer and a Nanospec interferometer calibrated with a standard sample to an accuracy within 5%. By x-ray photoluminescence spectroscopy (XPS), the chemical composition in the film is found to be 66.8% Si and 33.2% N in atomic weight.<sup>20</sup> Compared with 46.5% Si and 53.5% N in stoichiometric Si-N, Si-N films fabricated in present work are silicon enriched. Microstructures of these Si-N films, characterized by high-resolution electron microscopy (HREM), are seen to be amorphous in Fig. 2. It is also revealed that the 0.6- $\mu\text{m}$ -thick films are much more homogeneous than the 1.4- $\mu\text{m}$ -thick films, even though the deposition conditions are the same. The devices patterned on the film shown in Fig. 1 are made from tungsten strips which are 4  $\mu\text{m}$  in width and 0.2  $\mu\text{m}$  in height. The tungsten strip at the center of the thin film is used as a microheater. The second tungsten strip located 100  $\mu\text{m}$  from the heater is used as a sensor to detect the temperature at that position. The entire sample is covered with glass to prevent contamination from dust particles.

The sample is mounted on a circuit board in a vacuum chamber and the wires are connected to a feedthrough. The wires are shielded in order to reduce noise from the environment as well as the electrical interference among wires. The experimental setup consists of a constant current source for

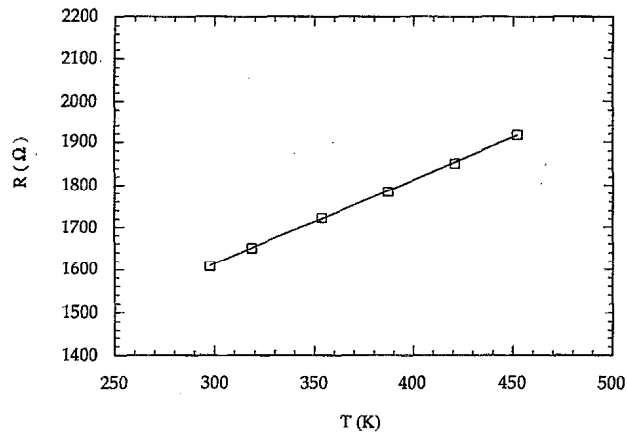


FIG. 3. Calibration of the microsensor resistance vs temperature.

the sensor, a SR510 lock-in amplifier, a HP 8116A function generator providing either an ac or dc current to the heater, a Tek11402 digitizing oscilloscope to monitor signals from both the heater and the sensor, and a computer data acquisition system. The simple constant current source is made from a 1.5 V dc battery and a few k $\Omega$  resistor. The sensor self-heating is minimized by using a small current of about 0.2 mA. The temperature change induced by self heating is estimated to be less than 0.8 K. This current varies less than 2% during the heating of the sensor up to 100 K above room temperature. The calibration of the sensor is carried out in an oven over the temperature range of 300–400 K. As indicated in Fig. 3, the sensor resistance increases linearly with increasing temperature. The vacuum chamber is pumped down to  $2 \times 10^{-5}$  Torr to eliminate possible convective heat losses from the free-standing thin film. Radiative heat losses are negligible, as the induced temperature in the thin film is less than 400 K. In order to enhance the signal-to-noise ratio, a large number of datasets are collected and averaged.

#### A. Thermal conductivity measurement

The steady heat flux in the range of  $10^5$ – $10^6$  W/m<sup>2</sup> is generated at the heater by a dc current from a function generator. The heater dc current and voltage, from which the heat flux can be found, are measured separately with a HP 3468A multimeter. At the beginning of the experiment, the sensor voltage is recorded as a baseline in the absence of heating of the thin film. After a heating current is applied to the heater, the sensor voltage change is measured. This voltage change can be converted into the temperature change  $\Delta T$  at the sensor using the constant current  $I$  and the calibration of  $R$ - $T$  in Fig. 3. Knowing the temperature increase  $\Delta T$ , heat flux  $q$ , film half length  $L$ , and sensor location  $X$ , the thin-film thermal conductivity can be found from Eq. (1). It should be pointed out, however, that the measured thermal conductivity corresponds to an average temperature between the heater and the sensor. This average temperature can be estimated as  $T_a = [(L - X/2)/(L - X)]T_s$ . To evaluate the thin-film thermal conductivity versus the temperature  $T_a$ , various heating fluxes are used by adjusting the heating current. The thin-film Si-N thermal conductivity dependence on temperature from 300 to 400 K is shown in Fig. 4.

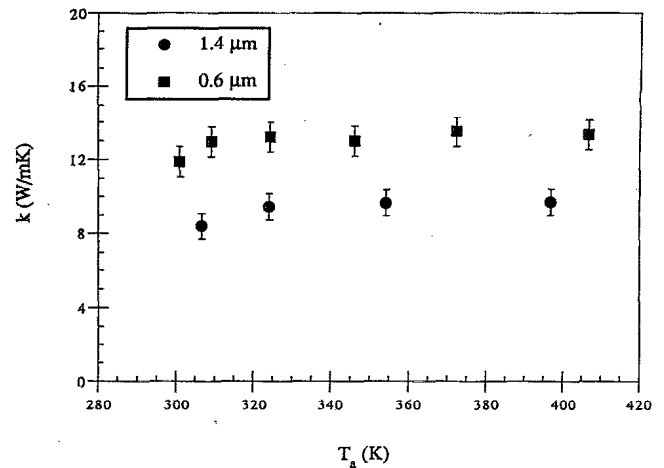


FIG. 4. Dependence of the thermal conductivity on temperature for Si-N film of 0.6 and 1.4  $\mu\text{m}$  in thickness.

#### B. Thermal diffusivity measured by the phase-shift method and the amplitude method

A periodic heat flux is generated at the center of the free-standing Si-N thin film in this experiment, by passing through the heater an ac current supplied by the function generator. The induced thermal wave traveling along the thin film is observed at the sensor. The equal heat fluxes are used for the experiments with both the 0.6 and the 1.4  $\mu\text{m}$  thin films. The phase shift between the sensor signals and the heating signals is measured by a lock-in amplifier with a phase error less than  $1^\circ$ . A multimeter is used to monitor the output of the lock-in amplifier. Phase shifts are measured in a frequency range from 80 to 200 Hz. In this frequency range, the sensor is located at a distance within one thermal wavelength from the heater. This is to eliminate any possible confusion by phase shifts out of  $2\pi$ . Figure 5 shows that the measured phase-shift changes linearly with the square root of the thermal wave frequency, for both the 0.6 and 1.4  $\mu\text{m}$  Si-N films. From the slope, the thermal diffusivities of two free-standing Si-N films can be determined according to Eq. (7). Simultaneously with the phase-shift measurement, the

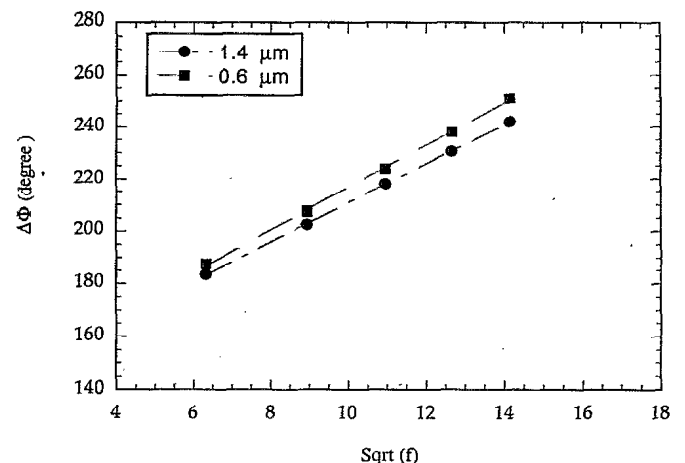


FIG. 5. Measured phase shift at the sensor location vs the square root of thermal wave frequency.

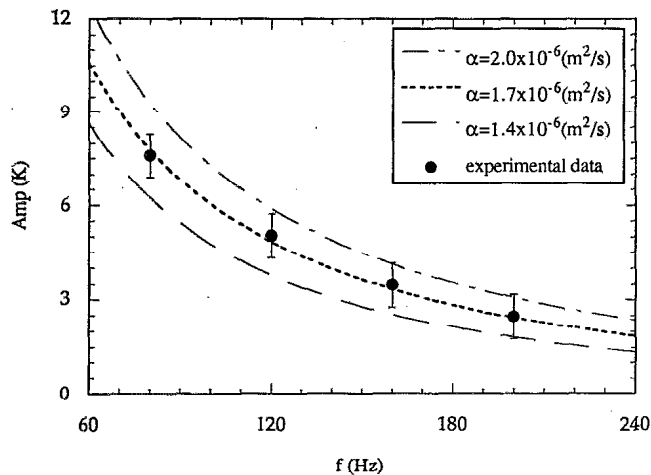


FIG. 6. Dependence of the thermal wave amplitude on the thermal wave frequency for the 0.6  $\mu\text{m}$  Si-N film.

amplitudes of thermal waves with different frequencies are recorded by the oscilloscope. The measured amplitude of the thermal wave decays as the frequency increases, as illustrated in Figs. 6 and 7. The best numerical fit to the experimental data is used to find the thermal diffusivities of the Si-N thin films. The envelope approximates the uncertainty in the measured thermal diffusivity.

### C. Thermal diffusivity measured by the heat pulse method

Heat pulses are produced by applying electrical pulses at the heater. The pulse width and magnitude can be adjusted incrementally with the function generator. Electrical pulses with the same width of 500  $\mu\text{s}$  but different magnitude are used to provide approximately equal heat fluxes for thin Si-N films with different thicknesses. Both the heating pulses and the sensing signals are acquired by the oscilloscope and transferred to a personal computer through a data acquisition interface. The heating pulse data are used as a time-scale reference in the subsequent analysis of the sensing signal.

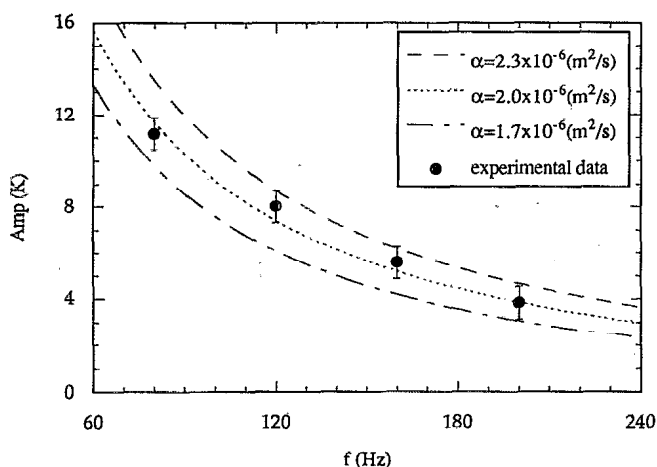


FIG. 7. Dependence of the thermal wave amplitude on the thermal wave frequency for 1.4  $\mu\text{m}$  Si-N film.

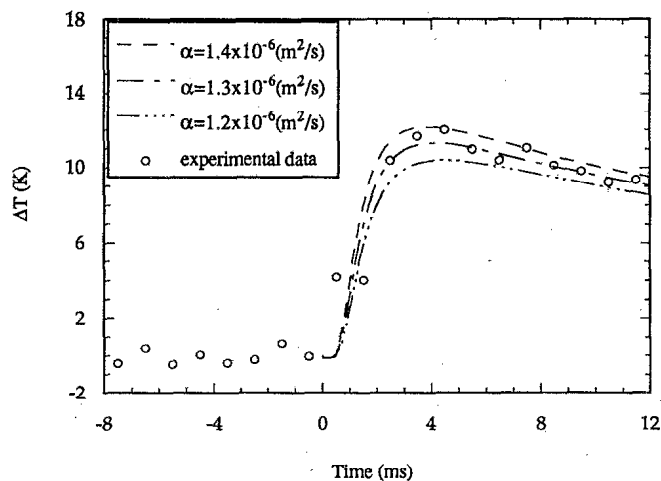


FIG. 8. Transient temperature profile at the sensor on the 0.6  $\mu\text{m}$  Si-N film, following a heat pulse of 500  $\mu\text{s}$  generated on the film.

Numerical fitting based on Eq. (13) gives the thermal diffusivities of the Si-N thin films as shown in Figs. 8 and 9.

## IV. RESULTS AND DISCUSSION

As seen in Fig. 4, the thermal conductivity of Si-N thin films is generally constant in the temperature range of 300–400 K. Measured thermal conductivities are about 9 W/mK for the 1.4  $\mu\text{m}$  film and 13 W/mK for the 0.6  $\mu\text{m}$  film. There are several sources of uncertainty in determining the thermal conductivity. The uncertainties in the film thickness of 5%, and in temperature measurements of  $\pm 1$  K, yield the experimental uncertainty in the measured conductivity about 10%. The thermal diffusivity of Si-N thin films is determined by three independent experiments: the phase-shift method, the amplitude method, and the pulse method. The results are summarized in Table I. From the slope of the phase shift with respect to  $\sqrt{f}$  in Fig. 5, the thermal diffusivities are found to be  $1.5 \times 10^{-6} \text{ m}^2/\text{s}$  for 0.6  $\mu\text{m}$  Si-N film and  $1.8 \times 10^{-6} \text{ m}^2/\text{s}$  for 1.4  $\mu\text{m}$  Si-N film. It is the advantage of the phase-shift method that the determination of the thermal diffusivity is

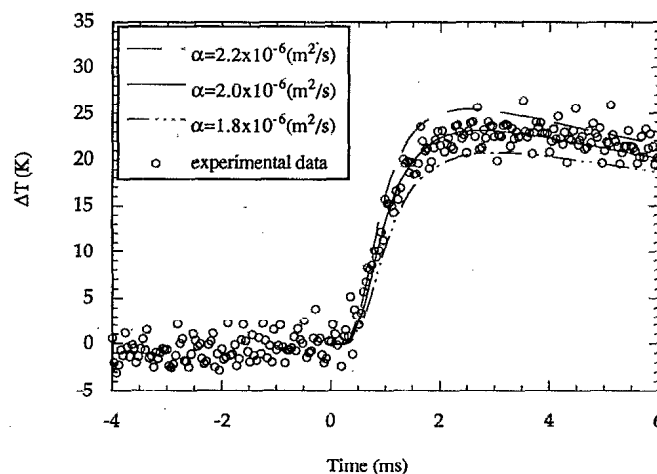


FIG. 9. Transient temperature profile at the sensor on the 1.4  $\mu\text{m}$  Si-N film, following a heat pulse of 500  $\mu\text{s}$  generated on the film.

TABLE I. Thermal diffusivities of Si-N thin films measured by three independent methods.

	Phase-shift method (m <sup>2</sup> /s)	Amplitude method (m <sup>2</sup> /s)	Heat-pulse method (m <sup>2</sup> /s)
0.6 μm film	(1.5±0.1)×10 <sup>-6</sup>	(1.7±0.3)×10 <sup>-6</sup>	(1.3±0.2)×10 <sup>-6</sup>
1.4 μm film	(1.8±0.1)×10 <sup>-6</sup>	(2.0±0.3)×10 <sup>-6</sup>	(2.0±0.2)×10 <sup>-6</sup>

independent of the thermal conductivity. From the signal-to-noise ratio of the sensor signal, combined with the resolution of the lock-in amplifier, it is assessed that the phase measurement is accurate within ±2°. The uncertainty in the distance between the sensor and the heater is about 1 μm. Frequencies are measured within ±0.1 Hz. The uncertainty in the measured thermal diffusivities by the phase shift method is found to be less than 10%. As shown in Figs. 6 and 7, the amplitude method determines the thermal diffusivities to be 1.7×10<sup>-6</sup> m<sup>2</sup>/s for the 0.6 μm film and 2.0×10<sup>-6</sup> m<sup>2</sup>/s for the 1.4 μm film. Determination of the film thermal diffusivity by the amplitude method requires knowledge of the thermal conductivity. The major sources of uncertainty in determining the thermal diffusivity by the amplitude method are the acquisition system resolution and the uncertainty in the measured thermal conductivity. The total uncertainty of the thermal diffusivity in the amplitude measurement is estimated to be 15%. As illustrated in Fig. 8 and Fig. 9, the thermal diffusivities of Si-N thin films obtained by the heat-pulse experiments are 1.3×10<sup>-6</sup> m<sup>2</sup>/s for the 0.6 μm film and 2.0×10<sup>-6</sup> m<sup>2</sup>/s for the 1.4 μm film. In order to reduce possible two-dimensional effects from the thin-film edges, the pulse duration is chosen as 0.5 ms and the sensor response is recorded over a time scale of 10 ms. The sensing signal noise and the uncertainty in the thermal conductivity are the two major factors causing the experimental error in the heat-pulse experiment. The total uncertainty in the determination of thermal diffusivities of Si-N thin films by the heat-pulse method is estimated to be about 15%. Good agreement on the thin-film thermal diffusivity measured by three independent experimental methods verifies the validity of the amplitude method which is proposed and implemented in present work. It also demonstrates that the amplitude method can be used as a new way of measuring the thin-film thermal diffusivity if its thermal conductivity is known, or obtaining the thermal conductivity if the thermal diffusivity is known.

It is interesting to note that the thermal conductivity of the thinner Si-N film (0.6 μm) is about 30% higher than that of the thicker Si-N film (1.4 μm). These two films were

deposited under the same conditions. HREM studies on the top surface region of the Si-N films reveal that the thinner film are much denser than the thicker films as shown in Fig. 2. A lot of small voids are found in the amorphous structure of the 1.4-μm-thick film while very few voids are found in the 0.6-μm-thick film. Therefore, it may be possible that the effective cross section area of the thicker film for the heat conduction is reduced by these voids. It is thus expected that the apparent thermal conductivity is lower. The above discussion is limited to qualitative explanation. More detailed statistical investigations of the microstructure of thin films and microscale thermal conduction analysis are required to draw quantitative conclusions.

## ACKNOWLEDGMENTS

Support by the National Science Foundation under Grant No. CTS-9210333 is gratefully acknowledged. The authors thank Xianfan Xu, Ted Bennett, Jeng-Rong Ho, Hee K. Park, and Yong Chen for their comments and technical help on this work. X. Z. also would like to thank James M. Bustillo of the Berkeley Sensor and Actuator Center (BSAC) of the University of California at Berkeley for providing valuable XPS data.

- <sup>1</sup>E. Paloura, K. Nauka, J. Lagowski, and H. C. Gatos, *Appl. Phys. Lett.* **49**, 97 (1986).
- <sup>2</sup>M. Maeda and H. Nakamura, *Thin Solid Films* **112**, 279 (1984).
- <sup>3</sup>G. W. Turner and M. K. Connors, *J. Electrochem. Soc.* **131**, 1211 (1984).
- <sup>4</sup>M. Moslehi, C. Y. Fu, T. W. Sigmon, and K. C. Saraswat, *J. Appl. Phys.* **58**, 2416 (1985).
- <sup>5</sup>A. J. Lowe, M. J. Powell, and S. R. Elliott, *J. Appl. Phys.* **59**, 1251 (1986).
- <sup>6</sup>A. S. Y. Ren and W. Y. Ching, *Phys. Rev. B* **23**, 5454 (1981).
- <sup>7</sup>R. M. Moroney, R. M. White, and R. T. Howe, *Appl. Phys. Lett.* **59**, 774 (1991).
- <sup>8</sup>S. W. Wenzel and R. M. White, *IEEE Trans. Electron Devices* **ED-35**, 735 (1988).
- <sup>9</sup>E. S. Kim, R. S. Muller, and P. R. Gary, *IEEE International Electron Devices Meeting*, Washington, D.C., 1989, p. 880.
- <sup>10</sup>F. R. Brotzen, P. J. Loos, and D. P. Brady, *Thin Solid Films* **207**, 197 (1992).
- <sup>11</sup>K. E. Goodson and M. I. Flik, *ASME, HTD* **253**, 29 (1993).
- <sup>12</sup>K. L. Saenger, *J. Appl. Phys.* **65**, 1447 (1989).
- <sup>13</sup>B. S. W. Kuo, J. C. M. Li, and A. W. Schmid, *Appl. Phys. A* **55**, 289 (1992).
- <sup>14</sup>D. G. Cahill, H. E. Fischer, T. Klitsner, E. T. Swartz, and R. O. Pohl, *J. Vac. Sci. Technol.* **7**, 1259 (1989).
- <sup>15</sup>Y. C. Tai, C. H. Mastrangelo, and R. S. Muller, *J. Appl. Phys.* **63**, 1442 (1988).
- <sup>16</sup>Y. Yu, X. Liu, Z. Fang, and S. Zou, *Appl. Surf. Sci.* **40**, 145 (1989).
- <sup>17</sup>S. Roy, S. Y. Bang, M. F. Modest, and V. S. Stubican, *Appl. Opt.* **32**, 3550 (1993).
- <sup>18</sup>I. Hatta, Y. Sasuga, R. Kato, and A. Maesono, *Rev. Sci. Instrum.* **56**, 1643 (1985).
- <sup>19</sup>W. P. Leung and A. C. Tam, *Opt. Lett.* **9**, 93 (1984).
- <sup>20</sup>J. M. Bustillo (private communication).